Received: 22 July 2021 | Revised: 18 September 2021 | Accepted: 29 September 2021

DOI: 10.1002/pol.20210576

RESEARCH ARTICLE

JOURNAL OF POLYMER SCIENCE WILEY

Single-chain polymers as homogeneous oxidative photoredox catalysts

Jacob J. Piane | Steven Huss | Lucas T. Alameda | Stephen J. Koehler | Lauren E. Chamberlain | Matthew J. Schubach | Ashley C. Hoover | Elizabeth Elacqua

Department of Chemistry, The Pennsylvania State University, University Park, Pennsylvania, USA

Correspondence
Elizabeth Elacqua, Department of Chemistry, The Pennsylvania State University, University Park, PA 18602, USA.
Email: elizabeth.elacqua@psu.edu

Funding information
Pennsylvania State University; National Science Foundation, Grant/Award Number: CHE-2046470

Abstract

Single-chain polymer nanoparticles (SCNPs) are emerging as versatile catalytic platforms that provide excellent control over solubility. The confined nature of SCNPs can improve the rate of catalysis. While significant headway has been made in thermally-induced transition-metal catalysis with SCNPs, light-activated SCNP catalysts have received little attention. We are developing triarylpyrylium tetrafluoroborate (TPT)-functionalized SCNPs as oxidative photocatalysts. Herein, we comprehensively study the impact of light source on both SCNP compaction and TPT absorbance through gel-permeation chromatography and UV/Vis spectroscopy. We observe that compaction is expedited using light sources that excite the photocatalyst (e.g., blue LEDs), which is attributed to the ability of TPT to dimerize sytrenics under similar photoredox conditions. The resultant metal-free SCNP photocatalysts enable the oxidation of benzyl alcohols in good yields. The SCNP is further investigated for the amidation of 4-bromobenzaldehyde, wherein it affords higher yields of the benzamide product compared to both small-molecule and unfolded polymer controls. We attribute the combined results to the colocalization of the TPT photoredox catalyst and pyrene electron relay within the SCNP, which likely aids in single-electron transfer processes. The scope of amidation reactions was also extended to other aryl aldehydes, wherein deactivated substrates afforded the highest yield of the desired amide.

KEYWORDS

catalysis, photoredox catalysis, single-chain polymer nanoparticles, triphenylpyrylium

1 | INTRODUCTION

Single-chain polymer nanoparticles (SCNPs) represent a class of nanomaterials consisting of intramolecularly cross-linked polymers.[1] The compartmentalized structure of SCNPs has inspired the development of drug delivery vehicles,[2] molecular sensors, and biomimetic catalysts.[3] The ability to tune the solubility of SCNPs with careful selection of comonomers addresses major bottlenecks in sustainable catalysis, including catalyst recovery and improved reactivity in aqueous media. Moreover, the substrate specificity that arises from the intrinsic properties of discretely-folded polymer nanoparticles, such as hydrophobicity and supramolecular binding cavities, is

Jacob J. Piane and Steven Huss these authors contributed equally.

reminiscent of enzyme catalysis.[4,5] The three-dimensional architecture of SCNPs allows catalysts to be placed in close proximity to one another in a single macromolecule, facilitating dual catalysis that can bypass the diffusion limitations inherent to small-molecule catalytic systems, with recent systems demonstrating accelerated reactivity in SCNPs in comparison to small molecule homogeneous catalysts.[6,7]

Significant progress has been realized in biomimetic and sustainable catalysis using transition metal cross-linked polymer nanoparticles wherein the metal creates a catalytic pocket within the macromolecule upon crosslinking. The Pomposo group demonstrated the unique ability of copper cross-linked SCNPs to selectively catalyze a Glaser-Hay homocoupling from a mixture of terminal alkynes.[8] Similarly, Lemcoff and coworkers demonstrated that high levels of selectivity between boronic acid homocoupling and cross-coupling may be achieved by manipulating the supramolecular architecture of rhodium SCNPs.[9] In 2017, Barner-Kowollik et al. leveraged the macromolecular architecture of SCNPs to realize a recyclable, homogeneous platinum catalyst for the amination of allyl alcohol.[10] More recent work by Zimmerman et al. demonstrated that Cu^{I}-SCNPs facilitated click reactions, wherein azides and alkynes diffuse into the interior of the polymer, proximal to Cu-binding sites. The "polymeric clickase" functioned to catalyze reactions of small molecules, as well as on proteins and within cells with accelerated rates when compared to small-molecule catalysts.[7] Moreover, a recent report of a frustrated Lewis acid/base polymer that undergoes chain collapse in the presence of CO_2 functions as a synthetic carboxylase. The CO_2-containing SCNP efficiently catalyzes the carboxylation of a diverse range of C—H bonds using CO_2 as a sustainable C_1 source.[11]

Photoredox catalysis has emerged as a powerful method for generation of radicals under mild reaction conditions.[12,13] Traditional methods for generating radicals rely on toxic and hazardous reagents such as organotin species and peroxides, or harsh conditions including high temperature and high energy UV irradiation. In contrast, photoredox catalysis enables the generation of a reactive radical species at ambient temperature without the use of harmful radical initiators upon visible light irradiation.[14,15] Palmans and coworkers utilized phenothiazine-functionalized amphiphilic SCNPs as photoredox catalysts as a stimuli-responsive catalytic platform that moves toward sustainable and biomimetic catalysis.[16] These reductive SCNPs were used for the metal-free dehalogenation of aryl halides. We recently reported photoredox cocatalytic SCNPs capable of metal-free dimerization of substituted styrene derivatives.[6] In these SCNPs, the polymer confinement accelerated single-electron transfer between cooperative catalysts, thus accelerating catalysis.

Herein, we present SCNP-based oxidative photoredox catalysts bearing visible-light-activated triphenylpyrylium (TPT) and further interrogate the crosslinking of styrylpyrene (SP) within the TPT-co-SP-co-MMA polymer, wherein different sources of light lead to various degrees of SCNP compaction, as evidenced by GPC and UV/Vis spectroscopy. For TPT-co-SP-co-MMA, lower energy light sources (e.g., blue lights) that were able to excite the TPT core led to faster single-chain collapse, likely owing to TPT facilitating the crosslinking process, given reports of it acting as a suitable photoredox catalyst in the dimerization of styrenics.[6,12,17] The TPT-SP-SCNPs served as efficient catalysts for the oxidation of benzyl alcohols under mild conditions. The synthetic utility of this transformation, in concert with the versatility of the SCNP photoredox catalyst, was further highlighted in a photocatalyzed-amidation of substituted aryl aldehydes, which proceed through a transient aminal intermediate and subsequent photocatalyzed-oxidation to yield the benzamide.

Triarylpyrylium salts are potent photooxidants, with an excited state potential of +1.9 V versus SCE for the parent compound 2,4,6-triphenylpyrylium tetrafluoroborate (TPT).[12] Triarylpyrylium salts are synthesized in one step from benzaldehydes and acetophenones, providing facile access to photocatalysts with varying electronic nature and therefore tunable redox potentials.[18] This, in conjunction with the absence of precious metals such as ruthenium and iridium that are present in many common photoredox catalyst systems, provides a highly tunable and sustainable platform for achieving photocatalyzed oxidations.

Key to our design is the use of SP as a tactical component; facile visible-light-mediated intramolecular crosslinking of SP-containing polymers at high concentrations relative to other crosslinking methods has been reported.[19] Given reports suggesting polycyclic compounds are broadly capable of acting as electron relay catalysts in photoredox systems,[17,20] we sought to introduce SP as a dual-functional unit. In our design, SP first partakes in covalent crosslinking to enable a confined SCNP structure, then subsequently acts as an electron relay catalyst in targeted photooxidative reactions.[6] Our strategy realizes an organocatalytic SCNP in which the two catalysts are colocalized within the same single-chain polymer framework, which acts to decrease the diffusion requirements inherent to small-molecule cocatalytic systems.

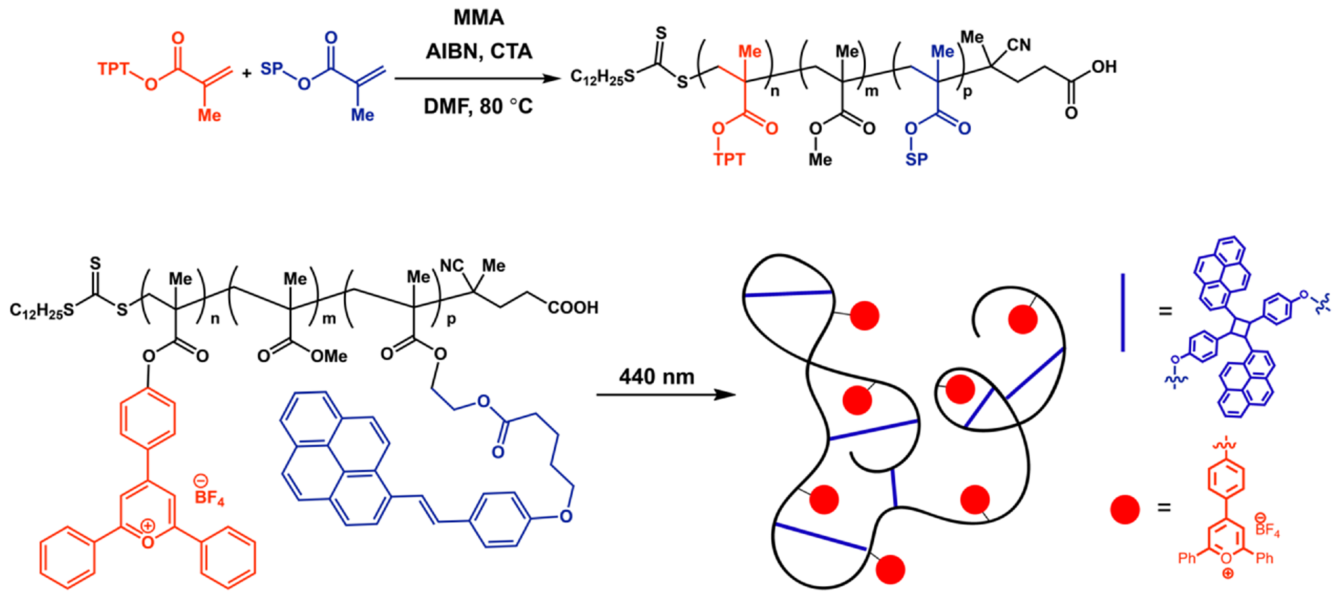

SCHEME 1 TPT-co-SP-co-MMA synthesis and folding to SCNPs through the [2 + 2] dimerization of SP pendants

2 | RESULTS AND DISCUSSION

A backbone of methyl methacrylate (MMA) was selected for the photocatalytic SCNPs to facilitate solubility in common organic solvents (e.g., MeCN, DCM). Polymers were prepared by reversible addition-fragmentation chain-transfer polymerization (RAFT, Scheme 1) with target incorporations of TPT and SP below 5%. Briefly, MMA, SP-methacrylate, and TPT-methacrylate were combined in dimethylformamide with AIBN as a radical source and 4-cyano-4-[(dodecylsulfanylthiocarbonyl) sulfanyl]pentanoic acid as the RAFT chain transfer agent. After sparging for 30 min, the reaction was heated at 80°C. After 24 h, the polymerization was quenched, and the resulting polymers were purified through reprecipitation in ether and methanol. The incorporation ratio of TPT and SP was determined by proton NMR spectroscopy, with characteristic, broad ether methylene peaks from SP at 4.26 ppm and 4.14 ppm and the methyl ester of MMA appearing at 3.55 ppm. The percent incorporation of TPT photocatalyst was determined by the remaining aromatic protons not attributed to SP. The resultant polymers were comprised of 1.9% TPT photocatalyst, 0.9% SP, and 97.2% MMA (Figure S1). Size-exclusion chromatographic analysis in THF revealed the polymer to be well-defined ($Đ = 1.20$) with a molecular weight of 24.7 kDa (Table 1).

We also synthesized three polymers using RAFT polymerization to assess if the folded SCNP has an impact on the targeted oxidative reactions. These polymers were prepared and characterized using ^{1}H-NMR spectroscopy and SEC (Table 1). The first polymer, TPT-co-MMA ($M_n = 15{,}200$; $Đ = 1.40$), contained 1.8% TPT by NMR spectroscopic analysis and, by design, no cocatalyst. The second polymer, TPT-co-MMA ($M_n = 9750$; $Đ = 1.19$), contained 17.2% TPT by NMR spectroscopic analysis and the third polymer, TPT-co-Py-co-MMA ($M_n = 16{,}700$; $Đ = 1.28$), has both TPT and pyrene catalysts in 1.6% and 0.5%, respectively; however, it would not be able to fold in a predictable manner to afford compartmentalized regions of catalyst. Together, both would aid in elucidating the role of the polymer folding on photoredox catalysis.

TABLE 1 Characterization for linear TPT-based polymers and SCNPs

Polymer	% TPT by NMR	% cocatalyst by NMR	M_n	M_w	$Đ$
TPT-co-SP-co-MMA	1.9	0.9	24,700	29,600	1.20
TPT-SP-SCNP	–	–	15,500	21,700	1.41
TPT-co-Py-co-MMA	1.6	0.5	16,700	21,400	1.28
TPT-co-MMA	1.8	N/A	15,200	17,900	1.17
TPT-co-MMA	16.0	N/A	9,750	11,700	1.19

2.1 | Formation of single-chain polymer nanoparticles

Prior reports of SCNPs featuring SP residues observed successful [2 + 2] dimerization using 430 nm irradiation, with timeframes and degree of compaction dependent on the molecular weights and degrees of SP incorporation within the MMA-based polymer. Recent reports have also observed successful SCNP formation through dimerization of SP using 470 nm light.[21] Similarly, our prior photoredox-active SCNPs were achieved by a [2 + 2] cyclodimerization of SP through irradiation with a white household CFL for 60–90 min.[6] Although this approach afforded SCNPs, as evidenced by combined gel permeation chromatography (GPC) and DOSY NMR spectroscopic measurements, we sought to further interrogate both light sources and irradiation times for dimerization keeping in mind that pronounced exposure to visible light could also lead to activation of TPT pendants. We, thus, investigated the use of 365 nm (common handheld TLC lamp), 427, 440, and 456 nm on the dimerization of our SP pendants in comparison to a white CFL lamp to elucidate which light source would be best for achieving compaction to SCNPs while not fully compromising the TPT chromophore. We hypothesized that those wavelengths which were also able to excite the TPT were likely to afford higher degrees of crosslinking, owing to the possibility that TPT could drive the [2 + 2] dimerization using a photoredox-initiated radical cation mechanism, as has been successfully observed in styrenics.[6,12,17]

Our initial studies screened all the light sources with the same approximate lamp-to-vial distances, using solutions of TPT-co-SP-co-MMA (M_n = 24,700; $Đ$ = 1.20) at 10 mg/mL in MeCN over a fixed period of 2 h with no stirring, followed by analyzing the crosslinking and TPT fidelity using GPC and UV/Vis spectroscopy. In all cases, successful crosslinking was confirmed by UV/Vis spectroscopy, wherein a decreased absorption was observed at 391 nm in the spectra, which can be attributed to a loss in conjugation upon dimerization (Figure 1). Additional distinct signals related to concomitant cyclobutane formation (λ = 333 nm and 352 nm) were observed in samples irradiated with the CFL lamp or 365 nm. In samples irradiated with 427, 440, or 456 nm, the overall absorbance profile decreases in intensity and broadens out, likely obscuring the cyclobutane features. Furthermore, after 2 h of irradiation, the overall absorbance of the TPT diminishes considerably, which can be attributed to photobleaching.

While the UV/Vis data confirmed successful crosslinking for all samples, GPC was used to gain further insights into the degree of intramolecular crosslinking and overall ability to form more compact SCNPs. Samples irradiated with either 365 nm or CFL lamps resulted in small shifts in molecular weight (ΔM_n < 6000) and their overall distributions suggested some degree of intermolecular crosslinking as evidenced by the appearance of a higher M_n tail in comparison to the sample prior to irradiation. In contrast, samples irradiated with 427, 440, or 456 nm showed very pronounced and complete shifts to lower molecular weights along with no visible signs of intermolecular crosslinking that confirmed higher degrees of compaction. The GPC data, combined with UV/Vis spectra obtained after irradiation suggested that wavelengths that also promote excitation of the TPT were advantageous for attaining higher degrees of compaction in SCNP formation.

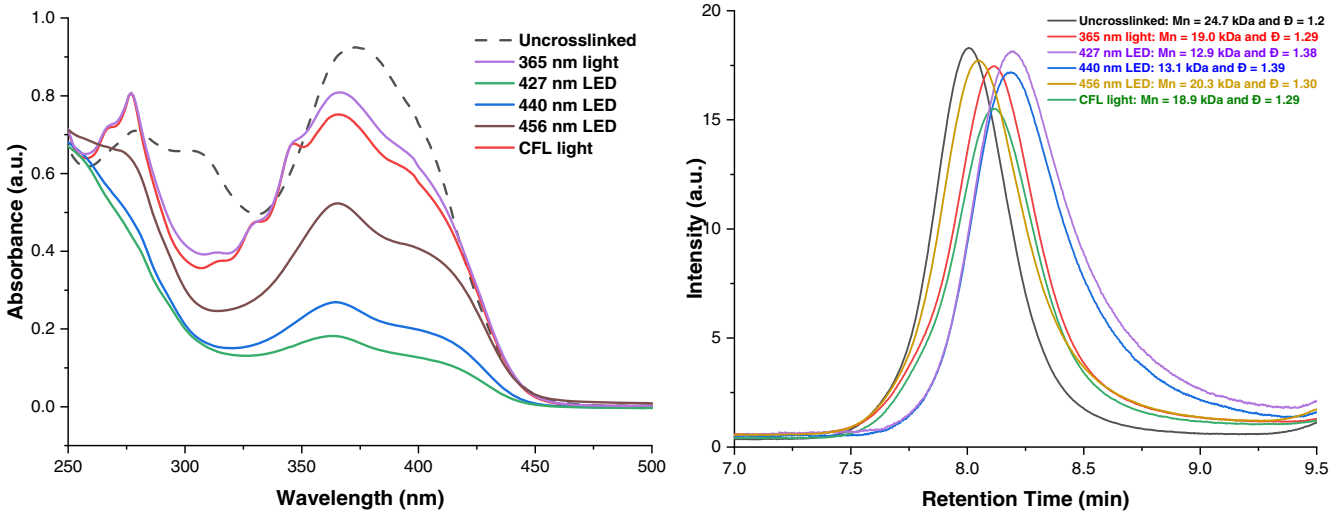

FIGURE 1 (left) UV/Vis spectral overlay and (right) SEC traces for TPT-co-SP-co-MMA after 120 min of exposure to different light sources to track the formation of TPT-SP-SCNPs

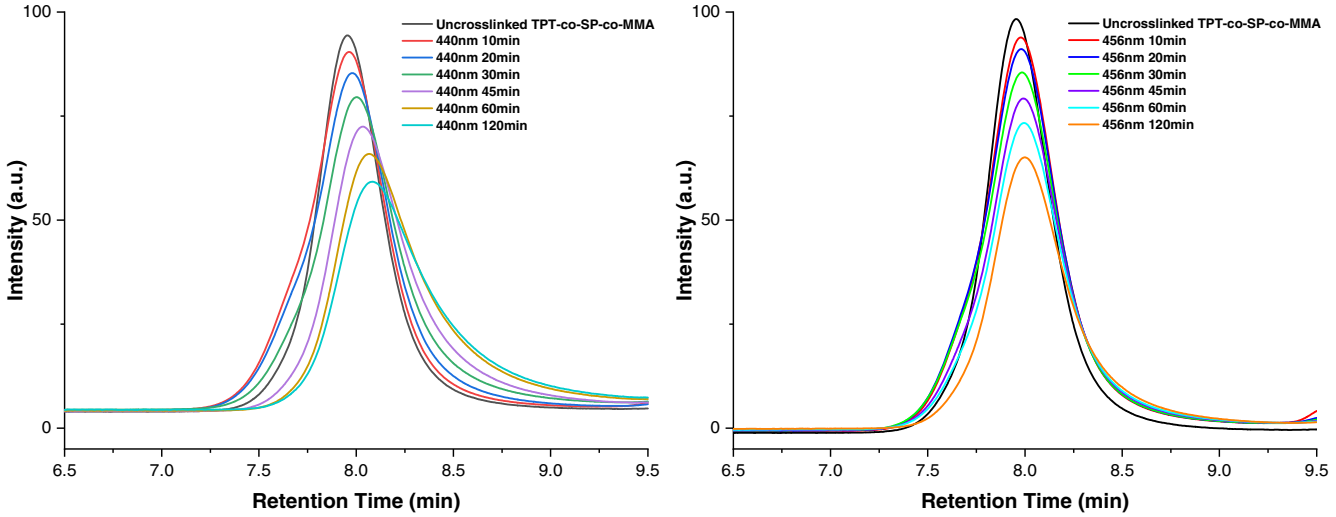

FIGURE 2 (left) SEC traces for TPT-co-SP-co-MMA upon irradiation with $\lambda = 440$ nm at different time intervals to follow the formation of TPT-SP-SCNPs and (right) SEC traces for TPT-co-SP-co-MMA upon irradiation with $\lambda = 456$ nm at different time intervals

We further probed the use of 440 and 456 nm light for SCNP formation, looking to identify irradiation times that would balance high degrees of compaction while retaining TPT absorbance (and thus, photoredox catalysis capability). TPT-co-SP-co-MMA ($M_n = 24{,}700$; $Đ = 1.20$) was irradiated with blue light in MeCN, wherein aliquots were drawn at 10, 20, 30, 45, 60, and 120 min for analysis of crosslinking using both UV/Vis spectroscopy and GPC. Generation of TPT-SP-SCNP using 440 nm light was evidenced as early as 10 min, wherein the UV/Vis spectrum featured the signature peaks ascribed to the cyclobutanes (Figure S8). These features were strong and consistent through 30 min, whereupon the overall absorbance profile broadened and the TPT profile decreased in intensity. Moreover, the GPC profile showed a consistent shifting to lower molecular weight as irradiation time increased. By 20 min of crosslinking, a decrease of ca. 3000 was noted, along with a small high molecular weight shoulder, suggestive of a small amount of uncontrolled crosslinking. On further irradiation to 30 min, that shoulder disappeared and a complete shift in the molecular weight distribution ($M_n = 18{,}800$ and $Đ = 1.39$) was observed. Extending irradiation to 45 and 60 min led to more compaction (45 min: $M_n = 15{,}500$ and $Đ = 1.41$; 60 min: $M_n = 12{,}900$ and $Đ = 1.49$)) (Figure 2).

Attempts to crosslink using 456 nm light did also lead to decreases in M_n over time; in contrast however, the overall process was much slower and only achieved a M_n of 21,600 within 60 min. Irradiation up to 2 h achieved a M_n of 20,300 ($Đ = 1.30$). Additional irradiation under 456 nm for up to 21 h, led to further compaction ($M_n = 13{,}200$ and $Đ = 1.38$; Figure S4), while crosslinking at 456 nm for 2 h at 100% light intensity also afforded high degrees of compaction ($M_n = 14{,}800$ and $Đ = 1.39$; Figure S4). Given the combined analyses, we chose to crosslink the polymer at 440 nm for 30–60 min since the decrease of molecular weight suggested effective SCNP formation while UV/Vis spectra in this timeframe (Figure S7) demonstrated that the TPT pendants still maintained moderate-to-strong absorbance and would be suitable for subsequent photoredox catalysis.

SEC confirmed intramolecular crosslinking of TPT-co-SP-co-MMA ($M_n = 24{,}700$; $Đ = 1.20$) upon exposure to 440 nm light to form TPT-SP-SCNP, which resulted in a distinct shift to lower molecular weight ($M_n = 15{,}500$ and $Đ = 1.41$). Successful folding was also confirmed using DOSY NMR spectroscopy. DOSY measurements on the unfolded TPT-co-SP-co-MMA revealed a coefficient of 2.11×10^{-10} m^2 s^{-1}. After exposure to 440 nm LEDs, a diffusion coefficient of 4.60×10^{-10} m^2 s^{-1} was observed, in line with successful compaction of SP pendant units through [2 + 2] dimerization.

2.2 | Oxidative photoredox catalysis

The synthetic utility of these polymer nanoparticles was first demonstrated in the oxidation of benzyl alcohols to the respective aldehyde or ketone (Figure 1). Using 1-phenylethanol as a model compound, we attempted the oxidation first using small molecule TPT in MeCN, both in the presence and absence of pyrene. After an hour of exposure to 427 nm Kessil lamps (2 at 100% intensity) in air, we obtained the product acetophenone in modest yields (36% with pyrene, 30% without pyrene) and with about 50% conversion of the starting alcohol. The slight increase in yield upon addition of pyrene might be owing

to the electron-accepting ability of pyrylium cations that facilitates formation of charge-transfer complexes with polycyclic aromatic hydrocarbons.[22] We then turned to using our TPT-SP-SCNP. In a typical experiment, the benzyl alcohol was added to a 0.03 M solution of the crosslinked TPT-SP-SCNP in a 20 mL vial in air, whereupon it was irradiated between two 427 nm Kessil lamps (100% light intensity) for 1 h, concentrated in the dark, and analyzed for conversion and yield through NMR spectroscopy. After assessing solvents at 1 mol % TPT-SP-SCNP loading, dichloromethane was found to be optimal for the oxidation (Table 2).

We found the oxidation of 1-phenylethanol to acetophenone proceeded in up to 67% yield using 7.5 mol% TPT-SP-SCNP (Table 2, bolded entry).[23] Longer reaction times and inert environments had deleterious effects on the yield of acetophenone. In the absence of light or polymer catalyst, trace amounts of product were observed. In prior reports of small-molecule TPT-photosensitized oxidation of methoxylated benzyl alcohols, additional oxidative byproducts were detectable.[24] Interestingly, analogous copolymers lacking SP pendants (TPT-co-MMA) or unable to fold (TPT-co-Py-co-MMA) were also able to oxidize the benzyl alcohol, albeit in lower overall yields, suggesting the SCNP interior is critical for the performance. We also found that using a TPT-co-MMA with a higher weight % of the photocatalytic unit decreased the overall yield.

Visible light photoredox catalysis using our TPT-based photocatalytic SCNPs enabled the oxidation of a variety of benzyl alcohols to the corresponding aldehyde or ketone in good yields. Substrates such as 4-chlorobenzyl alcohol and 4-methoxybenzyl alcohol proceeded in higher yield compared to the model phenylethanol. Methoxylated benzyl alcohols with *ortho* or *meta* substituents led to decreased yield, likely owing to lessened stability of the corresponding benzyl intermediates, consistent with prior reports of TPT-photosensitized oxidation of methoxylated benzyl alcohols.[24]

TABLE 2 Optimization table for the TPT-SP-SCNP-catalyzed oxidation of 1-phenylethanol to acetophenone

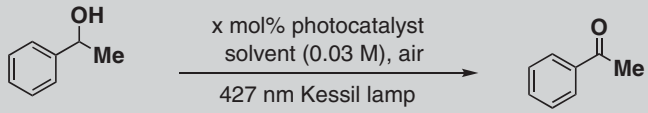

0.1 mmol

Photocatalyst	% PC (mol %)	Solvent	Light intensity	Time (min)	Yield[a] (%)
TPT	5	MeCN	100	60	30
TPT ((+) pyrene)	5	MeCN	100	60	36
TPT-SP-SCNP	5	MeCN	100	60	44
TPT-SP-SCNP	2.5	MeCN	100	60	32
TPT-SP-SCNP	1	MeCN	100	60	14
TPT-SP-SCNP	1	DCM	100	60	20
TPT-SP-SCNP	1	DME	100	60	4
TPT-SP-SCNP	1	Dioxane	100	60	<1
TPT-SP-SCNP	1	THF	100	60	2
TPT-SP-SCNP	**7.5**	**DCM**	**100**	**60**	**67**
TPT-SP-SCNP	7.5	$CDCl_3$	100	60	56[b]
TPT-SP-SCNP	7.5	$CDCl_3$	100	120	58[b]
TPT-SP-SCNP	7.5	$CDCl_3$	100	240	43[b]
TPT-SP-SCNP	7.5	DCM	0	60	2
None	N/A	DCM	25	60	1
TPT-co-MMA[c]	7.5	DCM	100	60	34
TPT-co-MMA[d]	7.5	DCM	100	60	5
TPT-co-Py-co-MMA	7.5	DCM	100	60	36

[a]Yields determined by ^{1}H-NMR spectroscopy using 1,3,5-trimethoxybenzene as an internal standard.
[b]The reaction was monitored by ^{1}H-NMR spectroscopy using 1,3,5-trioxane as an internal standard.
[c]Reaction conducted with TPT-co-MMA containing 8.3 wt % TPT.
[d]Reaction conducted with TPT-co-MMA containing 50 wt % TPT.

Our SCNP catalyst system can oxidize a variety of electron-rich benzyl alcohols in good yields, while more challenging electron deficient substrates such as 4-nitrobenzyl alcohol and 2,3,4,5,6-pentafluorobenzyl alcohol proceeded with decreased efficiency (Figure 3) likely owing to either an unfavorable oxidation (with respect to the excited state potential of TPT) or the possibility of the charge density of the radical cation mainly localizing in the aryl ring[24] rather than the benzyl position, preventing productive reactivity. In addition, for the anthracene methanol, the desired reaction competes with a favorable [4 + 4] dimerization which de facto leads to formation of a diol that would require different conditions to oxidize. Moreover, heteroaromatic substrates (e.g., pyridine, imidazole, and furan) did not lead to high amounts of the desired oxidation product, and in some cases led to insoluble polymer-like products being obtained. In the case of electron-rich primary benzyl alcohols, only the corresponding benzaldehydes were observed without any over-oxidation to the benzoic acid. These polymeric catalysts also facilitate the oxidation of secondary benzyl alcohols to their respective ketone. In all cases, we observed that the use of a 20 mL scintillation vial led to a higher yield in comparison to a 1 dram vial, which we ascribed to the greater amount of oxygen in the 20 mL vial owing to the headspace.

We hypothesized that the photocatalyzed oxidation of benzyl alcohols proceeds first through excitation of the pyrylium photocatalyst upon visible light irradiation. Pyrylium then activates the electron relay catalyst through a single electron oxidation, yielding pyrene cation radical as the active oxidant. Pyrene may then oxidize the benzyl alcohol to the corresponding arene cation radical, which is further oxidized to the desired benzaldehyde/ketone by oxygen. The role of oxygen was apparent from improved yields upon increasing the size of the reaction vessel. Upon oxidation with oxygen, hydrogen peroxide is generated in situ, which may also serve as an

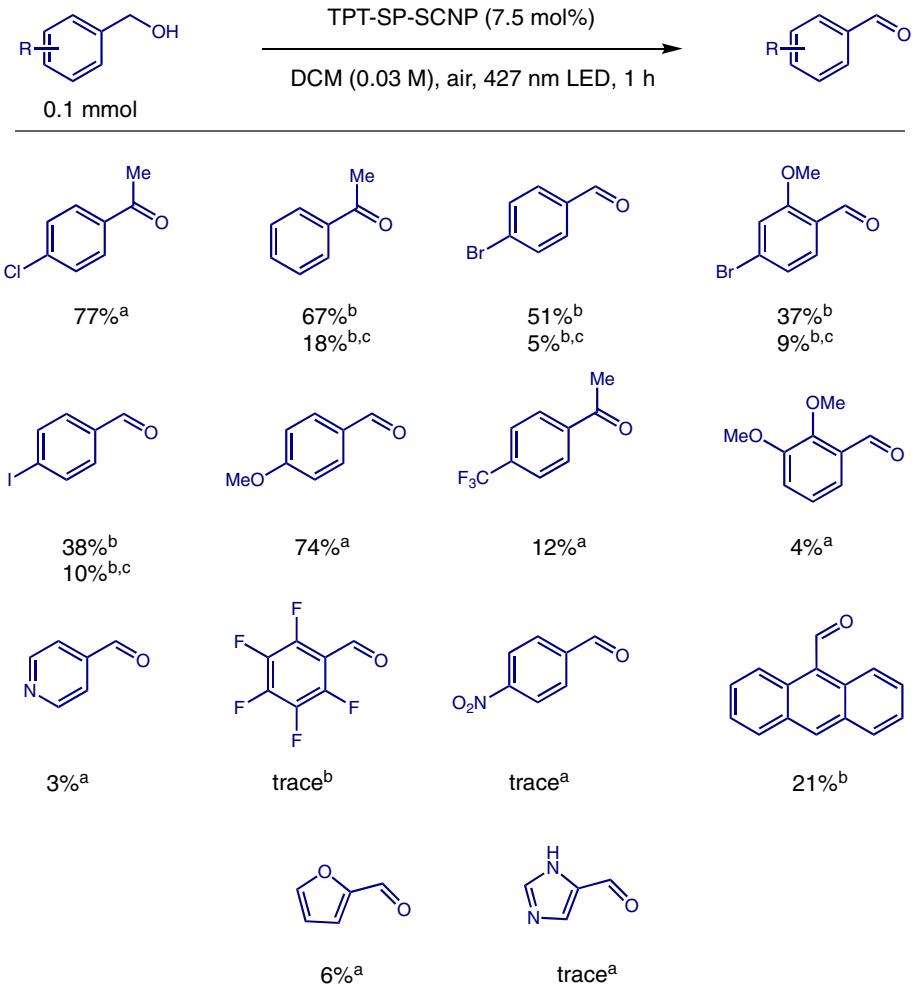

FIGURE 3 Scope of oxidation reactions of benzyl alcohols catalyzed by TPT-SP-SCNP

[a] Yields determined by ^{1}H NMR spectroscopy using 1,3,5-trioxane as an internal standard.
[b] Yields determined by ^{1}H NMR spectroscopy using 1,3,5-trimethoxybenzene as an internal standard.
[c] Reaction conducted in a 1 dram vial.

oxidant in this system. The resulting benzaldehyde cation radical then oxidizes reduced TPT to turn over the catalytic cycle and give the product (Figure 4).

To gain further insight to the plausibility of the proposed mechanism, we modeled the relevant molecules and intermediates. Time-dependent density functional theory (TD-DFT) using a ωB97X functional and 6-311G (d) basis set were used for both geometry optimizations and single point energy calculations (Figure 4).[25] Following the photoexcitation of TPT and intersystem crossing to its triplet state, the proposed single electron transfer with the pyrene electron relay is predicted to be energetically downhill, with a net gain of −60.94 kcal/mol. Subsequent oxidation of phenylethanol by the pyrene radical cation is also favorable and predicted to net −26.25 kcal/mol. Finally, the reduction of the resulting aldehyde by the TPT radical is also favorable, resulting in a net of −30.59 kcal/mol. Thus, the overall proposed mechanism is energetically favorable after excitation of TPT.

Intrigued by the oxidation results, we postulated that a photocatalyzed-amidation proceeding through a transient aminal intermediate was possible. The reported photocatalyzed oxidative amidation of benzaldehyde occurs using a phenazine-based photocatalyst.[26] Given the higher oxidation potential of pyrylium-based organic photoredox catalysts, we examined the possibility that the small molecule could also catalyze the amidation reaction (Table S3). Using 4-bromobenzaldehyde and pyrrolidine with 5 mol % *p*-tol TPT in MeCN, we irradiated the sample with blue LEDs and obtained a conversion of 84%, but only a 49% yield of the amidation product. We hypothesized that the addition of a polyaromatic hydrocarbon could work to increase the product yield by acting as an electron relay. Addition of anthracene afforded up to 60% of the amidation product when using 0.5 equivalents of the cocatalyst.

With successful formation of the amide product from small-molecule visible light photoredox catalysis, we then turned our attention toward utilizing our TPT-SCNP to facilitate the reaction. Given the colocalization of the PC and ER catalysts, we envisioned the SCNP might be able to promote more efficient electron transfer for the reaction. Indeed, the visible-light-catalyzed amidation of 4-bromobenzaldehyde with pyrrolidine using the TPT-SP-SCNP (5 mol %)[23] affords the benzamide in up to 89% yield (Table 3, bolded entry). Moreover, significant degrees of the amide product (75–80%) are observed even with as little as 10 min of crosslinking (i.e., less compact SCNP), while the

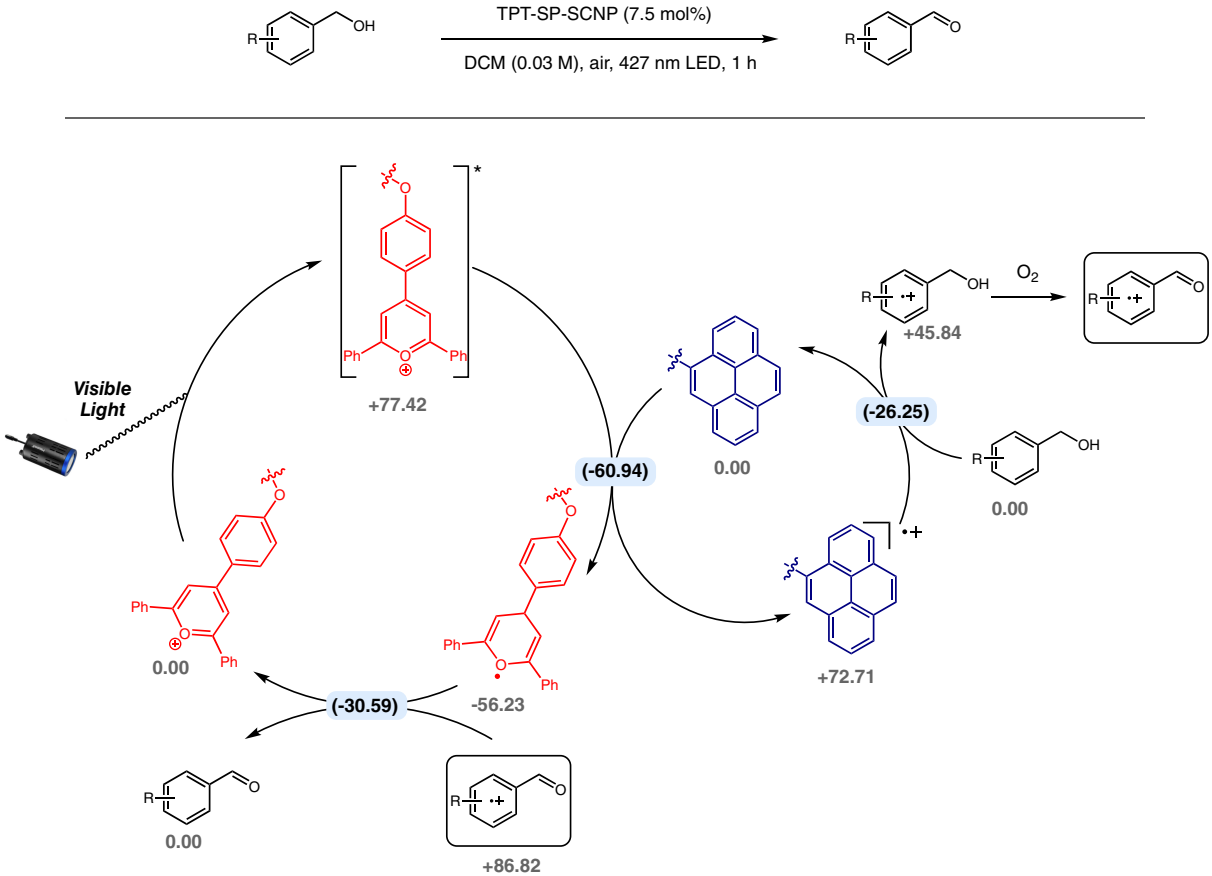

FIGURE 4 Proposed mechanism for the TPT-SCNP photocatalyzed oxidation of benzaldehydes with associated relative energies (kcal/mol) calculated using TD-DFT (ωB97X/6-311G(d))

TABLE 3 Optimization table for the SCNP catalyzed amidation of 4-bromobenzaldehyde

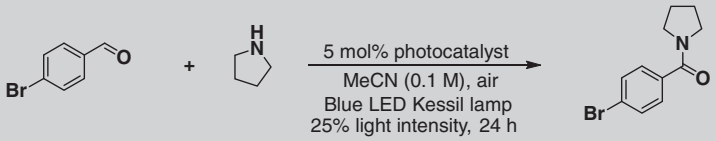

Photocatalyst	Electron relay	Light source (nm)	Yield (%)
TPT-SP-SCNP	TPT-SP-SCNP	427	75
TPT-SP-SCNP	**TPT-SP-SCNP**	**440**	**89**
TPT-SP-SNCP	TPT-SP-SCNP	456	78
TPT-SP-SCNP (N_2 Sparged)	TPT-SP-SCNP	427	48
TPT-SP-MMA	TPT-SP-MMA	427	78
TPT-SP-SCNP	TPT-SP-SCNP	none	12
TPT-co-MMA (8.3 w%)	None	427	43
TPT-co-MMA (50 w%)	None	427	65
TPT-co-Py-co-MMA	TPT-co-Py-co-MMA	427	32

smaller SCNPs afford 89% of the benzamide (Table S4). Reactions conducted in the absence of light or SCNP did not afford any of the desired amidation product. Reactions run without air also resulted in an overall lessened yield. In contrast, small molecule TPT and small molecule pyrene, untethered to each other in any way, afforded the benzamide in 29% yield (Table S3).

When the PC and ER catalysts were unconfined, the benzamide yield was significantly decreased using our prior optimized conditions. Linear TPT-co-Py-co-MMA, which incorporated both the PC and ER catalysts, but without the capacity for proximal confinement, afforded the benzamide in 32% yield, despite a 95% conversion of aldehyde. Similarly, TPT-co-MMA in the absence of any additive performed akin to the small molecule TPT, affording 43% of the amide product. Utilizing TPT-co-MMA with a higher amount of TPT in the backbone allowed for a 65% yield to be obtained. Combined, the

FIGURE 5 Scope of amidation reactions of aromatic aldehydes catalyzed by TPT-SP-SCNP

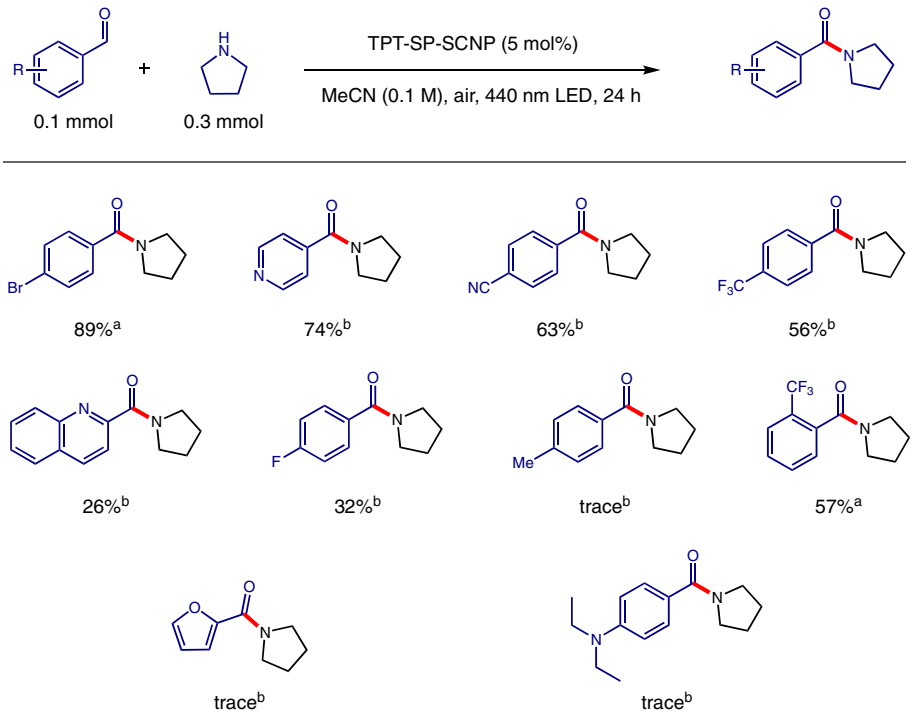

[a] Yields determined by ^{1}H NMR spectroscopy using 1,3,5-trimethoxybenzene as an internal standard.
[b] Yields determined by ^{1}H NMR spectroscopy using 1,3,5-trioxane as an internal standard.

results suggest that the single-chain form of the TPT photocatalyst acts to overcome diffusion limitations between the photocatalyst and electron relay within the loosely-confined interior. Thus, the amidation reaction with the SCNP catalyst likely triggers more efficient single-electron transfer between catalysts.

Using the optimal conditions, other aromatic aldehydes were interrogated for reaction with pyrrolidine in the presence of TPT-SP-SCNP as the photoredox catalyst (Figure 5). Consistent with prior reports on organic photoredox catalyzed oxidative amidation, aldehydes containing electron-withdrawing groups resulted in more efficient reactions compared to those with electron-donating groups.[26] Specifically, substrates such as 4-pyridinecarboxaldehyde, 4-(trifluoromethyl)benzaldehyde, and 4-cyanobenzaldehyde resulted in moderate to high yields of the aromatic amide (Figure 5). Moreover, changing the substitution pattern from *para* to *ortho* for (trifluoromethyl)benzaldehyde had insignificant effects on reactivity, suggesting crowding around the reaction center did not deter reactivity. Near complete conversion of the aldehyde was detected with most substrates used, with other oxidative products (e.g., substituted benzoic acids and other unidentified side products) being detected through mass spectrometry with electronically-activated systems.

3 | CONCLUSIONS

In summary, we studied MMA-based polymers bearing light-activated TPT and SP pendants. The [2 + 2] dimerization of SP pendants was investigated comprehensively using a series of light sources. We found that blue LEDs which simultaneously trigger photoexcitation of the TPT units enabled SCNP formation in a more expedited fashion and demonstrated more pronounced shifts to lower molecular weights on compaction compared to white lights or UV sources. We attributed this to the ability of the TPT moiety to promote the radical cation-based dimerization of styrenes. The more compact SCNPs were used for homogeneous oxidative photoredox catalysis, wherein the oxidation of benzyl alcohols proceeded without over oxidation. Furthermore, the single-chain polymers were capable of catalyzing the amidation of deactivated aryl aldehydes in up to 89% yield. These TPT-based SCNP catalysts leverage the confined nature of the intramolecularly-crosslinked architecture with proximally located photoredox and electron relay catalysts to enhance reactivity. This enhancement was observed in the amidation reaction of 4-bromobenzaldehyde, which proceeded with higher yield of product in comparison to both small molecules and polymer systems that were not able to achieve a compartmentalized structure. Moreover, the TPT-SP-SCNP facilitated the amidation of electronically-deactivated aryl aldehydes. Future work will focus on investigating other SCNP photocatalysts for their ability to promote enhanced reactivity while leaning toward sustainable catalysis.

4 | EXPERIMENTAL SECTION

All chemicals were purchased from Sigma Aldrich, Alfa Aesar, Oakwood Chemicals, or TCI America, and used as received unless otherwise indicated. NMR spectroscopic characterization was conducted on a Bruker Avance 500 or 400 MHz spectrometer using $CDCl_3$ unless otherwise indicated. Chemical shifts are reported in ppm, and referenced to residual $CHCl_3$. Trioxane was utilized as an internal standard for conversion and yields of small-molecule transformations. Polymer molecular weights and dispersities were measured using a TOSOH EcoSEC HLC-8320 GPC, coupled UV and RI detectors, controlled by an EcoSEC-WS program, and calibrated with poly(styrene) standards. The column and guard column utilized were pre-packed from TOSOH in THF (TSKgel GMHHR-H; mixed bed column, 7.8 mm I.D. × 30 cm) and the column temperature was maintained at 24 °C. All samples were measured with a THF mobile phase (Sigma-Aldrich, HPLC grade, inhibitor free). The injection volume was 8 μL and the flow rate was 1 mL min^{-1}. UV–visible absorption spectra were obtained on an Agilent Cary 60 UV–visible spectrophotometer (Agilent Technologies, Inc) using a quartz cuvette (Starna Cells). Polymer solutions for UV–Vis analysis were prepared in acetonitrile (Sigma-Aldrich, HPLC grade).

Photoredox experiments were conducted using Kessil LED photoredox lights (427 nm or 440 nm; PR160) using either 20 mL scintillation vials or 1 dram vials pending reaction scale. All reactions were irradiated using two Kessil PR 160 LEDs at a vial-to-lamp distance of 6.5 cm with a cooling fan positioned either adjacent to the reactions (household desk fan) or above the reactions. More information and specifics can be found at: http://www.kessil.com/science/resources.php.

Experimental procedures and characterization data for all monomers and polymerization procedures have been reported previously.[6]

Molecules were modeled using TD-DFT with Orca computational software version 5.0.1. Each of the molecules were simulated using a conductor-like polarizable continuum model (CPCM) with dichloromethane as a solvent to mimic reaction conditions. Each of the molecules were optimized using an ωB97X functional and 6-311G(d) basis set, tight convergence criteria, and

numerical frequency calculations to confirm an energy minimum was achieved. An ester was added to the top of the TPT to best mimic the PMMA backbone. A cyclobutyl substituent was appended from the electron relay, pyrene, to simulate the cyclized dimer present in the reaction conditions. The substrate, phenylethanol, and its oxidized form were unmodified.

4.1 | General procedure for oxidation reactions

The benzyl alcohol (0.1 mmol) was added to a 20 mL foil wrapped scintillation vial containing the SCNP (0.0075 mmol). DCM (3.75 mL) was added in the dark. The foil was removed and the vial was then irradiated with two Kessil lamps for 1 h. The sample was then concentrated in the dark. Trimethoxybenzene or trioxane was added and the yield was calculated by ^{1}H-NMR spectroscopy.

4.2 | General procedure for amidation reactions

The SCNP (33.3 mg, 0.005 mmol) in a 10 mg/mL solution of MeCN was added to a 20 mL scintillation vial and concentrated. The aldehyde (0.1 mmol) was added followed by pyrrolidine (0.025 mL, 0.3 mmol). The contents of the vial were dissolved in MeCN (1 mL) and then the vial was stirred between two Kessil lamps for 24 h with a cooling fan. The vial was concentrated and an internal standard was added. The yield was then calculated by ^{1}H-NMR spectroscopy.

ACKNOWLEDGMENTS

This work was supported by the National Science Foundation Early CAREER program (CHE-2046470). The authors also acknowledge support from start-up funds generously provided by the Pennsylvania State University. L.E.C. acknowledges financial support in the form of a Charles P. and Dorothy A. Neidig Scholarship, as well as an undergraduate Erickson Discovery Grant and Benkovic Summer Fellowship. We further acknowledge Sarah Freeburne for GPC sample collections.

ORCID

Elizabeth Elacqua https://orcid.org/0000-0002-1239-9560

REFERENCES

[1] C. K. Lyon, A. Prasher, A. M. Hanlon, B. T. Tuten, C. A. Tooley, P. G. Frank, E. B. Berda, *Polym. Chem.* **2015**, *6*, 181.
[2] A. Latorre-Sánchez, J. A. Pomposo, *Polym. Int.* **2016**, *65*, 855.
[3] J. Rubio-Cervilla, E. González, J. A. Pomposo, *Nanomaterials* **2017**, *7*, 341.
[4] J. Chen, E. S. Garcia, S. C. Zimmerman, *Acc. Chem. Res.* **2020**, *53*, 1244.
[5] H. Rothfuss, N. D. Knöfel, P. W. Roesky, C. Barner-Kowollik, *J. Am. Chem. Soc.* **2018**, *140*, 5875.
[6] J. J. Piane, L. E. Chamberlain, S. Huss, L. T. Alameda, A. C. Hoover, E. Elacqua, *ACS Catal.* **2020**, *10*, 13251.
[7] J. Chen, J. Wang, K. Li, Y. Wang, M. Gruebele, A. L. Ferguson, S. C. Zimmerman, *J. Am. Chem. Soc.* **2019**, *141*, 9693.
[8] A. Sanchez-Sanchez, A. Arbe, J. Colmenero, J. A. Pomposo, *ACS Macro Lett.* **2014**, *3*, 439.
[9] S. Mavila, I. Rozenberg, N. G. Lemcoff, *Chem. Sci.* **2014**, *5*, 4196.
[10] N. D. Knöfel, H. Rothfuss, J. Willenbacher, C. Barner-Kowollik, P. W. Roesky, *Angew. Chem., Int. Ed.* **2017**, *56*, 4950.
[11] R. Zeng, L. Chen, Q. Yan, *Angew. Chem., Int. Ed.* **2020**, *59*, 18418.
[12] N. A. Romero, D. A. Nicewicz, *Chem. Rev.* **2016**, *116*, 10075.
[13] K. L. Skubi, T. R. Blum, T. P. Yoon, *Chem. Rev.* **2016**, *116*, 10035.
[14] D. M. Arias-Rotondo, J. K. McCusker, *Chem. Soc. Rev.* **2016**, *45*, 5803.
[15] L. Buzzetti, G. E. M. Crisenza, P. Melchiorre, *Angew. Chem., Int. Ed.* **2019**, *58*, 3730.
[16] F. Eisenreich, E. W. Meijer, A. R. A. Palmans, *Chem. Eur. J.* **2020**, *26*, 10355.
[17] M. Riener, D. A. Nicewicz, *Chem. Sci.* **2013**, *4*, 2625.
[18] A. Vega-Peñaloza, J. Mateos, X. Companyó, M. Escudero-Casao, L. Dell'Amico, *Angew. Chem., Int. Ed.* **2021**, *60*, 1082.
[19] H. Frisch, J. P. Menzel, F. R. Bloesser, D. E. Marschner, K. Mundsinger, C. Barner-Kowollik, *J. Am. Chem. Soc.* **2018**, *140*, 9551.
[20] T. Tamai, N. Ichinose, T. Tanaka, T. Sasuga, I. Hashida, K. Mizuno, *J. Org. Chem.* **1998**, *63*, 3204.
[21] H. Frisch, D. Kodura, F. R. Bloesser, L. Michalek, C. Barner-Kowollik, *Macromol. Rapid Commun.* **2020**, *41*, 1900414.
[22] M. A. Miranda, H. García, *Chem. Rev.* **1994**, *94*, 1063.
[23] We note that the actual mol % of active TPT is far lower, owing to a high degree of the TPT absorbance being quenched in the crosslinking process (See Figures S7–9).
[24] B. Branchi, M. Bietti, G. Ercolani, M. A. Izquierdo, M. A. Miranda, L. Stella, *J. Org. Chem.* **2004**, *69*, 8874.
[25] Calculations were completed using Orca 5.0.1 computational software. The energies for electron transfers were calculated with the assumption that they are adiabatic processes.
[26] D. Leow, *Org. Lett.* **2014**, *16*, 5812.

SUPPORTING INFORMATION

Additional supporting information may be found in the online version of the article at the publisher's website.

How to cite this article: J. J. Piane, S. Huss, L. T. Alameda, S. J. Koehler, L. E. Chamberlain, M. J. Schubach, A. C. Hoover, E. Elacqua, *J. Polym. Sci.* **2021**, *59*(22), 2865. https://doi.org/10.1002/pol.20210576